$Co_xFe_{3-x}O_4$," *J. Phys. Chem. Solids*, **37**, 619–24 (1976).
[9]J. F. Sarver, "Compound Formation and Phase-equilibrium Relationships in the Systems CoO-P_2O_5 and NiO-P_2O_5," *Trans. Br. Ceram. Soc.*, **65**, 191–98 (1966).
[10]J. C. Kaell, F. Jeannot, and C. Gleitzer, "Study of the Progressive Reduction of $Fe_3(PO_4)_7$ and $Fe_9(PO_4)O_8$" (in Fr.), *Ann. Chim. (Paris)*, **9** [2] 169–80 (1984).
[11]A. Modaressi, J. C. Kaell, B. Malaman, R. Gérardin, and C. Gleitzer, "Study of the System Fe-P-O (for Fe/P ≥ 1) and its Compounds: The Oxyphosphates of Iron" (in Fr.), *Mater. Res. Bull.*, **18**, 101–109 (1983).
[12]M. Bouchdoug, A. Courtois, R. Gérardin, J. Steinmetz, and C. Gleitzer, "Preparation and Study of an Oxyphosphate $Fe_4(PO_4)_2O$" (in Fr.), *J. Solid State Chem.*, **42**, 149–57 (1982).
[13]A. Modaressi, A. Courtois, R. Gérardin, B. Malaman, and C. Gleitzer, "Fe_2PO_5, a Mixed Valence Iron Phosphate. Preparation and Structural, Mössbauer, and Magnetic Studies" (in Fr.), *J. Solid State Chem.*, **40**, 301–11 (1981).
[14]G. Venturini, A. Courtois, J. Steinmetz, R. Gérardin, and C. Gleitzer, "Preparation and Study of a Mixed-Valence Iron Oxyphosphate $Fe_9(PO_4)O_8$" (in Fr.), *J. Solid State Chem.*, **53** [1] 1–12 (1984).
[15]A. Modaressi, A. Courtois, R. Gérardin, B. Malaman, and C. Gleitzer, "Fe_3PO_7, a Case of 5-Coordinated Trivalent Iron. Structural and Magnetic Studies" (in Fr.), *J. Solid State Chem.*, **47**, 245–55 (1983).
[16]J. Korinth and P. Royen, "Reactions in the System Fe_2O_3/$FePO_4$" (in Ger), *Z. Anorg. Allg. Chem.*, **313** [3–4] 121–37 (1961).
[17]Yu. Gorbunov, B. Maksimov, Yu. Kabalov, A. Ivashchenko, O. Mel'nikov, and N. Belov, "Crystal Structure of $Fe_3^{2+}Fe_4^{3+}(PO_4)_6$," *Dokl. Akad. Nauk SSSR*, **254**, 873–77 (*Sov. Phys. Dokl.* (Eng. Transl.), **25** [10] 785–87) (1980).
[18]H. Wentrup, "Contribution on the System Iron-Phosphorus-Oxygen" (in Ger.), *Arch. Eisenhüttenwes.*, **9** [7] 57–60 (1935).
[19]E. C. Shafer, M. W. Shafer, and R. Roy, "Studies of Silica Structure Phases II. Data on $FePO_4$, $FeAsO_4$, $MnPO_4$, BPO_4, $AlVO_4$, and Others," *Z. Kristallogr.*, **107**, 263–75 (1956).
[20]D. W. Collins, G. E. Rindone, and L. N. Mulay, "Search for Superparamagnetism in the Iron Phosphate System," *J. Am. Ceram. Soc.*, **54** [1] 52 (1971).
[21]M. D. Dyar, "Precision and Interlaboratory Reproducibility of Measurements of the Mössbauer Effect in Minerals," *Am. Mineral.*, **69**, 1127–44 (1984).
[22]C. Greaves and R. G. Burns, "Correlations of Infrared and Mössbauer Site Population Measurements of Actinolites," *Am. Mineral.*, **56**, 2010–33 (1971).
[23]A. J. Stone, K. A. Parkin, and M. D. Dyar, "STONE: A Program for Fitting Mössbauer Spectra," Digital Equipment Corporation User's Society Publication No. 11–270. Marlboro, MA, 1984.
[24]R. G. Burns and V. M. Burns, "Crystal Chemistry of Meteoritic Hibonites," *J. Geophys. Res.*, **89**, Supplement, C313–C321 (1984).
[25]R. H. Vogel and B. J. Evans, "Solid-State and Magneto-Chemistry of the SrO-Fe_2O_3 System—III. The Non-Existence of Single-Phase '$SrFe_2O_4$,'" *J. Magn. Magn. Mater.*, **13**, 294–300 (1979). □

J. Am. Ceram. Soc., **70** [11] 837–42 (1987)

Spinel Phase Formation During the 980°C Exothermic Reaction in the Kaolinite-to-Mullite Reaction Series

BIROL SONUPARLAK,*,* MEHMET SARIKAYA,* and ILHAN A. AKSAY*

Department of Materials Science and Engineering, College of Engineering, University of Washington, Seattle, Washington 98195

With the use of differential thermal analysis, X-ray diffraction, and transmission electron microscopic techniques, we showed that γ-Al_2O_3 type spinel phase is solely responsible for the 980°C exotherm in the kaolinite-to-mullite reaction series. Transmission electron microscopic characterization indicated that the spinel formation is preceded by a phase separation in the amorphous dehydroxylated kaolinite matrix. Chemical analysis of the spinel phase by energy dispersive X-ray spectroscopy revealed a nearly pure Al_2O_3 composition.

I. Introduction

THE kaolinite ($Al_2O_3 \cdot 2SiO_2 \cdot 2H_2O$)-to-mullite ($3Al_2O_3 \cdot 2SiO_2$) reaction series has been the subject of various studies for nearly a century,[1] and still retains its active status as evidenced in most recent publications.[2–7] However, these studies have not resolved the questions concerning the issue of which phase formation is responsible for the exothermic reaction commonly observed at around 980°C.

The first step in the reaction series is the formation of an amorphous dehydration product identified as metakaolinite ($Al_2O_3 \cdot 2SiO_2$) after an endothermic reaction at ≈550°C. In the next step, the formation of crystalline product(s) from this amorphous intermediate phase results in a prominent exothermic reaction at ≈980°C. In most studies[3–17] dealing with this reaction series, the key issue has been the identification of the reaction product that results in this exothermic reaction.

The reaction mechanisms proposed for the 980°C exotherm can be classified into two general groups. In the first group, the common feature is the formation of a γ-Al_2O_3 type spinel phase and its association with the exothermic reaction.[3–5,8,9,13–17] The differences reported are mainly concerned with the composition of the spinel phase and whether the mullite phase (through a parallel reaction) also contributes to the exotherm.[3,14,16] In contrast to these spinel-based models, the second group proposes the formation of mullite without any spinel phase.[10–12] In view of the convincing evidence presented in recent studies,[3,14–16] the validity of this second mechanism can now be disputed.

With respect to the spinel-based mechanisms, however, two key problems still remain on the issues of (1) whether the spinel or the mullite phase is responsible for the exothermic reaction at 980°C and (2) how much silicon, if any, is present in the spinel phase. In this paper, we provide the answer to the first of these questions. We show that the spinel phase alone is responsible for the exothermic reaction. We also provide a partial solution to the second question, showing that this spinel contains <10 wt% silica and is probably very close to being pure alumina.

II. Experimental Procedure

Well-crystallized kaolinite† was used in all our experiments. Based on chemical analysis and structural analysis by X-ray diffraction, 1.39 wt% TiO_2 was identified as the main impurity.[17]

Presented at the 37th Pacific Coast Regional Meeting of the American Ceramic Society, San Francisco, CA, October 30, 1984 (Basic Science Division, Paper No. 55-B-84P). Received October 27, 1986; revised copy received May 18, 1987; approved May 27, 1987.
Supported by the Defence Advanced Research Projects Agency of the Department of Defence and monitored by the Air Force Office of Scientific Research under Grant No. AFOSR-83-0375.
*Member, the American Ceramic Society.
*Now with Advanced Materials Division, Flow Industries, Inc., Kent, WA 98032.
†Georgia Kaolinite (KGa-1), Georgia Kaolin Co., Elizabeth, NJ.

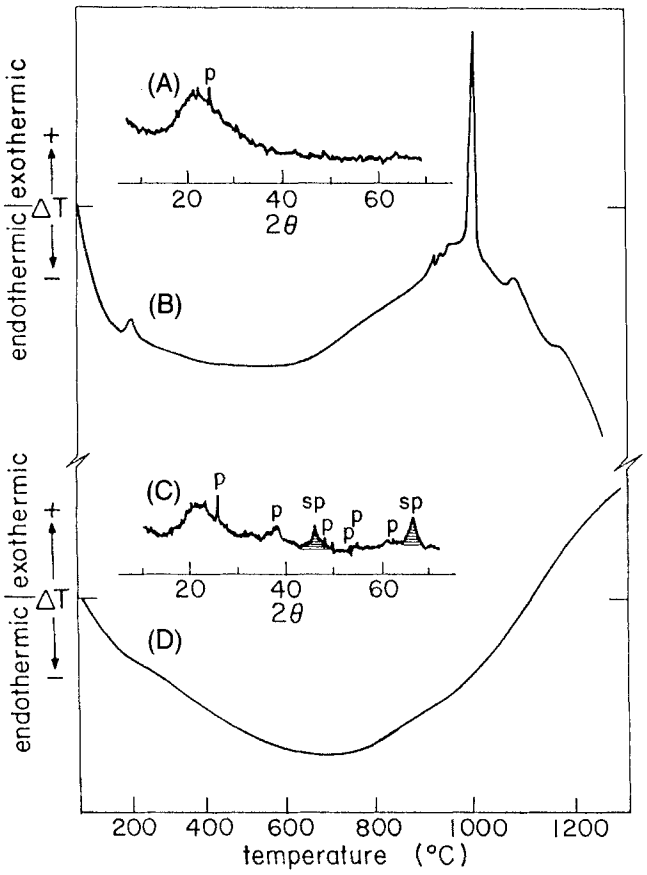

Fig. 1. X-ray diffraction ((*A*) and (*C*)) and differential thermal analysis ((*B*) and (*D*)) patterns of kaolinite after an isothermal heat treatment at 850°C for 1 d ((*A*) and (*B*)) and 7 d ((*C*) and (*D*)). In the XRD patterns, pseudoanatase and spinel peaks are labeled as *p* and *sp*, respectively.

Differential thermal analysis (DTA)[‡] studies were performed in air, at a heating rate of 10°C/min, up to 1250°C. In addition, isothermal heating studies were performed at various temperatures below the exothermic peak temperature for up to 7 days in a resistance-heated furnace. Phase characterization was performed by X-ray (Cu$K\alpha$) diffraction (XRD). Detailed descriptions of the experimental conditions related to XRD and DTA are given elsewhere.[17] In situ beam-induced heating experiments in a transmission electron microscope (TEM)[§] and high-resolution electron microscopy (HREM)[¶] were performed in order to observe the phase changes directly. Chemical analyses of the phases were performed by utilizing energy dispersive X-ray spectroscopy (EDS).** Special powder samples were prepared by heat-treating the original kaolinite at temperatures below the 980°C exothermic reaction and by treating it with 10 wt% boiling NaOH solution at different periods of time up to 40 min. Amorphous silica-rich phase was dissolved during this NaOH treatment, allowing more accurate evaluation of the chemical composition of the spinel crystals which are not soluble under these conditions. The Cliff-Lorimer method[18] was used to obtain quantitative analysis of the X-ray spectra. Kaolinite was used as a standard in the determination of $k_{Al,Si}$. All data for quantitative analysis were acquired by tilting specimens 30° toward the detector. Data were acquired in a multichannel scaler set in the 10-kV range. Si_K (at 1.74 kV) and Al_K (at 1.48 kV) peaks were separated by using 250-eV energy windows. In all cases, powder samples for TEM characterization were suspended on a holly carbon film attached on a 75-mesh Cu grid.

[‡]Du Pont 900 thermal analyzer, E.I. du Pont de Nemours & Co., Wilmington, DE.
[§]Philips 400 EM, Philips Electronics Inc., Mahwah, NJ.
[¶]JEOL 200CX, JEOL USA, Inc., Peabody, MA.
**KEVEX 7000, KEVEX Co., Foster City, CA.

III. Results and Discussion

(1) Formation of Spinel Phase

XRD analysis of the DTA samples heated to or above the exothermic reaction temperature always indicated the formation of the spinel phase along with mullite. This concomitant existence of spinel with mullite led previous investigators[3,14,16] to the conclusion that both of these phases may be responsible for the exothermic reaction. Therefore, in order to determine if the formation of these phases could be separated from each other, we isothermally heat-treated kaolinite at various temperatures lower than the exothermic peak temperature. In doing so, it was assumed that only one of the phases would be obtained at a given temperature and thus the contribution of this phase to the reaction would result in a decrease in the exothermic peak intensity in a subsequent run.

As expected, when kaolinite was subjected to heat treatment at 850°C, the spinel phase formed before mullite. Figures 1(*A*) and (*C*) show the XRD patterns obtained after heat treatment for 1 and 7 d at 850°C, respectively. After a 1-d heat treatment, only the formation of pseudoanatase, $2Al_2O_3 \cdot 2TiO_2 \cdot SiO_2$ (labeled *p*), and a large amount of an amorphous phase was observed (Fig. 1(*A*)). Our calculations indicated that the TiO_2 impurity may result in the formation of 2.46 wt% pseudoanatase. A large amount of an amorphous phase is also expected, because metakaolinite contains 51.61 wt% SiO_2 and as explained below most of this component segregates as a silica-rich phase during the heat-treatment process. Extended (7-d) heatings at 850°C resulted in the development of the spinel phase without any mullite (Fig. 1(*C*)). The DTA curves of these 1- and 7-d heat-treated samples are shown in Figs. 1(*B*) and (*D*), respectively. A significant difference is observed between the two samples. While the exothermic reaction is observed in the DTA curve for the 1-d heat-treated sample (Fig. 1(*B*)), it is completely eliminated in the second DTA trace (Fig. 1(*D*)). In spite of the differences in the DTA curves, upon further heating, mullite formation is observed to the same degree in both samples. However, since mullite is formed through a diffusion-controlled reaction in the second case, its formation is not easily observed in the DTA trace (Fig. 1(*D*)). This behavior and the information obtained from the XRD analyses clearly lead us to conclude that the spinel phase alone is responsible for the exothermic reaction.

Further evidence supporting this conclusion was obtained through beam-induced in situ heating experiments performed in a TEM. Although in the in situ experiments the exact temperature of the samples could not be measured, approximate temperature ranges could be determined through comparison of the microstructures with those of ex situ ones. Three different characteristic stages were observed (Fig. 2). The bright-field (BF) image in Fig. 2(*A*) was taken after the dehydroxylation had started. The formation and growth of light-color patchy regions are interpreted to be associated with the loss of structural water. After the completion of this dehydroxylation process, the structure was determined to be amorphous by electron diffraction. The image in Fig. 2(*B*) was taken upon further heating, but to a temperature low enough so that crystallization would not occur. Careful inspection of this figure reveals a structure similar to that obtained in spinodally decomposed systems. Further heating to a higher temperature first resulted in the growth of these phase-separated regions and then the formation of a crystalline phase took place. As revealed in the bright- and dark-field (DF) pairs of Figs. 2(*C*) and (*D*), respectively, the size of the crystalline regions was ≈5 to 8 nm. Although we could not obtain isolated electron diffraction patterns, the analysis of the superimposed patterns indicated only the presence of a cubic spinel type phase but not mullite. This observation then also supports the view that spinel and mullite phases do not form in parallel reactions. spinel formation takes place first, after a phase separation process in the metakaolinite.

In order to unambiguously determine that the crystalline phase formed at the 980°C reaction belongs to a spinel phase, we attempted to grow larger spinel crystals on which electron micro-

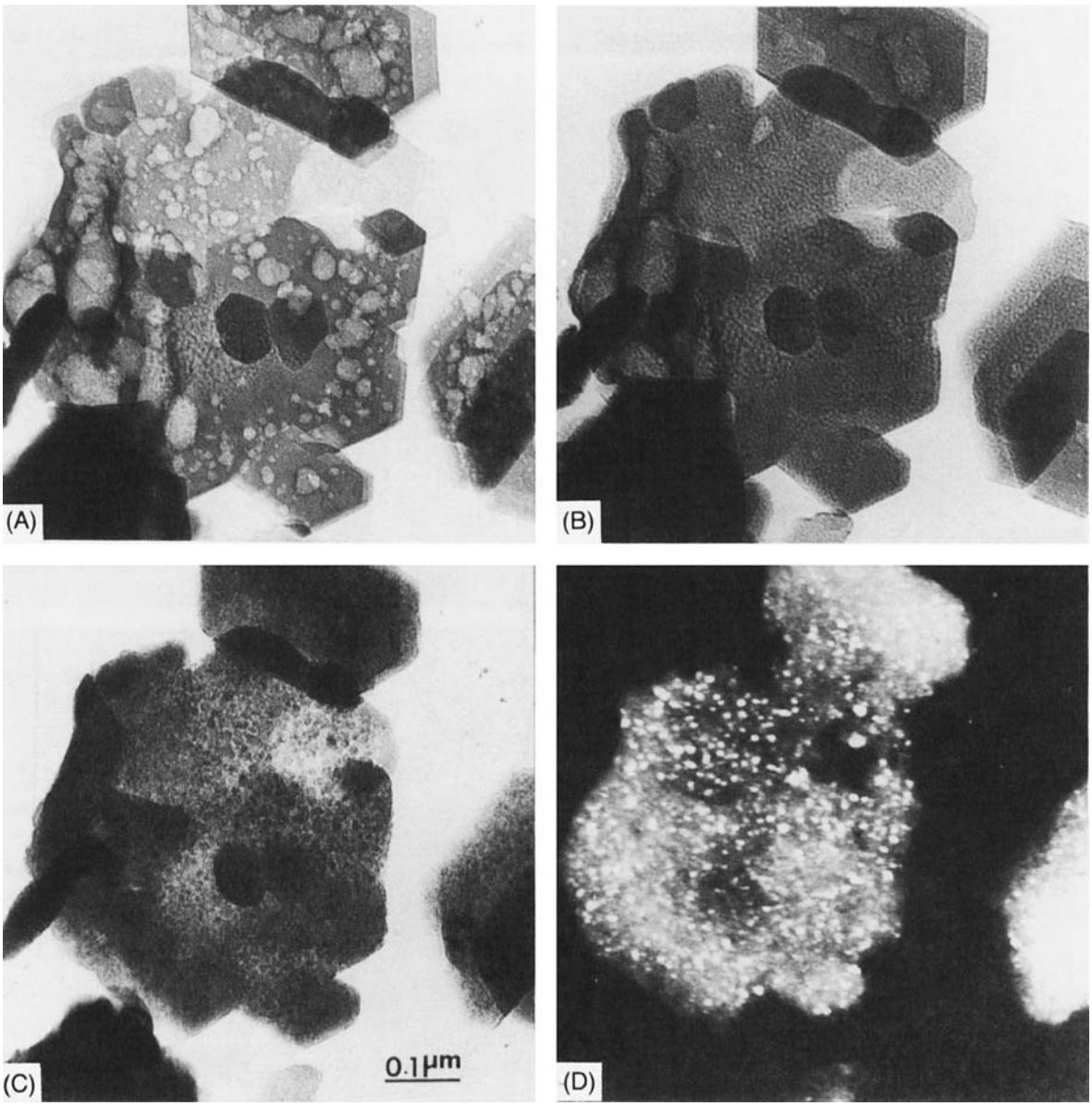

Fig. 2. Morphological changes that take place in kaolinite during electron-beam-induced in situ heating experiments: (*A*) BF image revealing the microstructure during dehydroxylation; (*B*) microstructure of metakaolinite before the 980°C exothermic reaction; (*C*, *D*) BF and DF images, respectively, which reveal the spinel crystallites in an amorphous matrix.

diffraction experiments would be performed to obtain isolated diffraction patterns. For this purpose, samples were externally heated at prolonged times (1 d) at temperatures near but below the exothermic reaction. As illustrated in the TEM images of Fig. 3, we were successful in growing the spinel grains to sizes larger than 100 nm. The bright-field (BF) image in Fig. 3(*A*) from a corner of a particle indicates variations in the structure resembling a contrast associated with a crystalline area. In fact, the corresponding dark-field (DF) image in Fig. 3(*B*) clearly reveals the morphology of the crystalline region which is surrounded by an amorphous phase at the edge of the particle. Microdiffraction patterns were received from this region by using an electron beam 40 nm (400 Å) in diameter. The microdiffraction pattern in Fig. 3(*C*) corresponds to a $\langle 114 \rangle_{fcc}$ zone axis orientation. The specimen was further tilted to another orientation, now near $\langle 122 \rangle_{fcc}$ to unambiguously confirm the *fcc* structure of the spinel phase. Similar experiments were also performed on another spinel crystal ($FeZnO_3$) which was used as a standard for comparison.

The growth pattern of the spinel phase was evidenced from the high-resolution images taken at high enough magnifications to reveal the crystallographic planes of the spinel grains (Fig. 4). There are several image features worthwhile to describe here in studying the formation and the growth of the spinel phase at small scale. Firstly, in Fig. 4(*A*), two sets of Moiré fringes are revealed on the lower part of the micrograph, indicating that there are two thin layers of crystals situated on top of each other possibly with an amorphous layer in between. This indicates that spinel phase grows in layers within an amorphous structure. There is only one layer, however, near the edge of the particles as indicated by *CF* and *LF* (corresponding to cross fringes and lattice fringes, respectively) where the thickness of the region in the electron beam direction should be considerably small. Another important image feature is the appearance of the very small regions, 1.5 to 4.0 nm in diameter (as indicated by black arrows), in Fig. 4(*B*). These small crystallites are forming in the amorphous matrix near the edge of the particles. They exhibit similar lattice spacing with the larger crystallites, such as the region on the lower left of the same micrograph, where the phase front (indicated by fat arrows) advances toward the small crystallites probably joining with them eventually and extending the spinel region all the way to the edge.

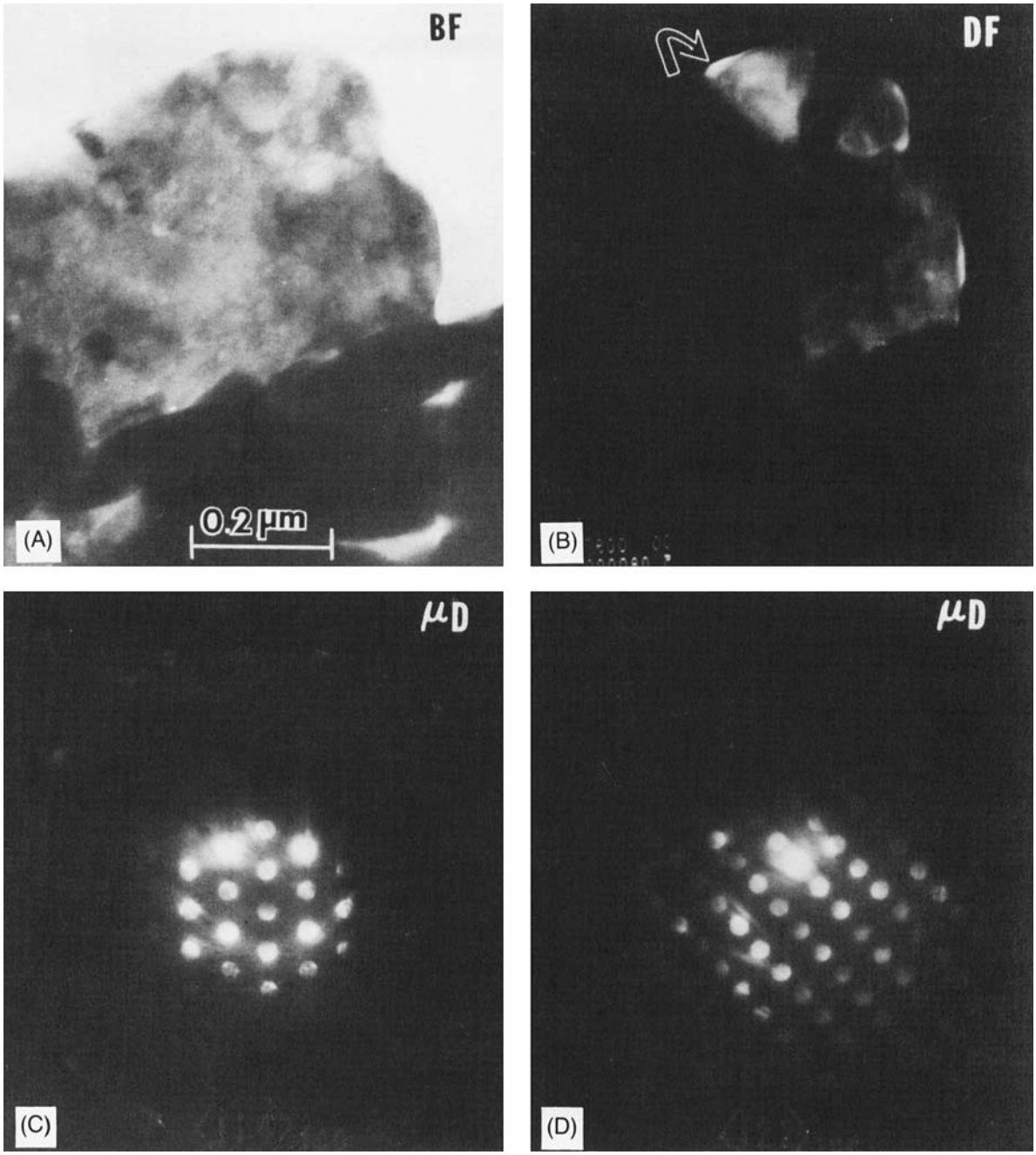

Fig. 3. Spinel phase grown at ≤980°C for 1 d: (*A*, *B*) BF and DF images, respectively, revealing the morphology; (*C*, *D*) microdiffraction patterns near $\langle 114 \rangle_{fcc}$ and $\langle 122 \rangle_{fcc}$ zone axis orientations, respectively.

(2) Composition of the Spinel Phase

The observation of the spinel phase alone in an amorphous matrix, during in situ heating experiments, led us to design another experiment to answer the second question associated with the composition of the spinel phase. In previous studies[13–16] the composition of this phase was always determined through indirect analyses. However, direct compositional analysis is now possible by EDS in an analytical TEM if the spinel phase is physically isolated from the surrounding amorphous phase. For this purpose, the spinel-containing samples, which were produced by extending heating (7 d) at 850°C, were treated with 10 wt% boiling NaOH. As a result, the bulk of the amorphous phase was leached out, gradually leaving the spinel crystallites intact (Fig. 5). These figures are directly comparable with the images presented in Fig. 2(*B*), where the spinel phase was formed by beam heating. The original shape of the kaolinite crystals is still retained. Because of the leaching of the SiO_2-rich amorphous phase from the bulk of the platelets, the images exhibit a contrast resembling a porous structure.[19] Direct microanalysis was performed by EDS on the clusters of crystallites after different leaching times to measure the amount of Al and Si from which the amounts of Al_2O_3 and SiO_2 would be calculated. Figure 6 illustrates the results of the analysis where the amount of SiO_2 is plotted with respect to leaching time. The analysis of this plot indicates that at extended leaching times (>25 min) the rate of leaching of SiO_2 approaches zero below 10 wt% SiO_2. It is important to point out that during the leaching process, the spinel crystals appeared to be unaffected visually. Their XRD patterns were also not different compared to the unleached and 40-min-leached samples. This indicates that neither the particle size nor the composition of the spinel was

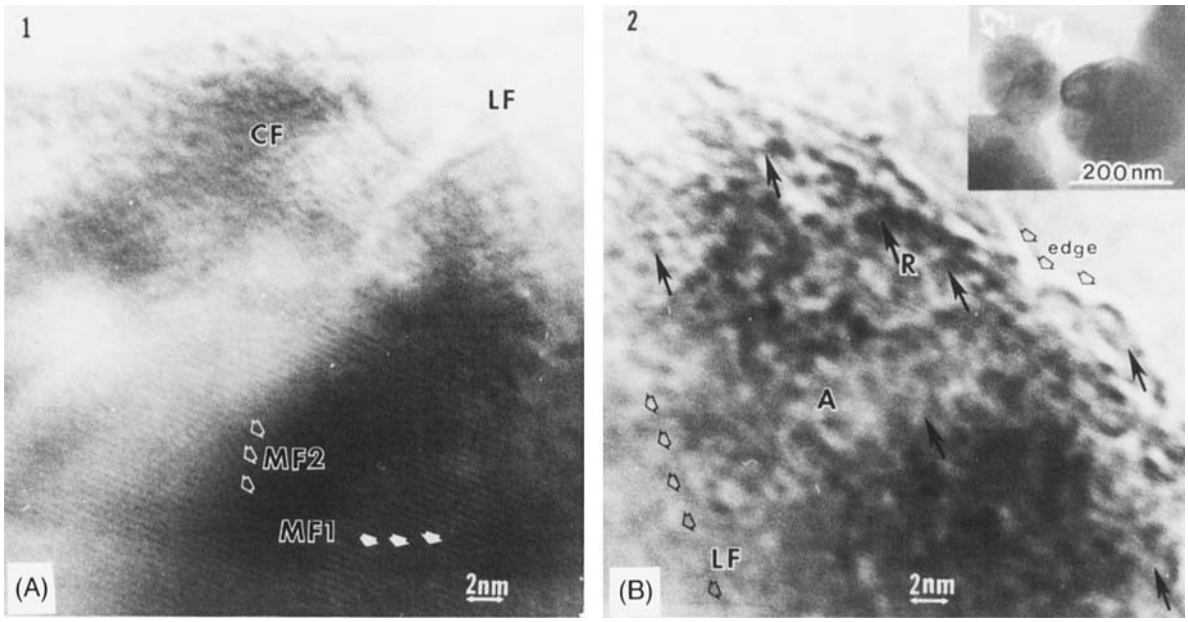

Fig. 4. High-resolution images of a sample heated at ≤980°C for 1 d. Images (*A*) and (*B*) were taken from regions *1* and *2*, respectively, of the crystal shown in the inset. In (*A*), two sets of Moiré fringes (indicated by *MF1* and *MF2*) are shown suggesting layers of crystals. In regions indicated by *CF* (cross fringes) and *LF* (lattice fringes), there is only one layer. In micrograph (*B*) beyond the phase front (between the spinel and the amorphous matrix), there are small crystallites (patchy regions with cross fringes indicated by the black arrows near the edge) forming in the amorphous phase.

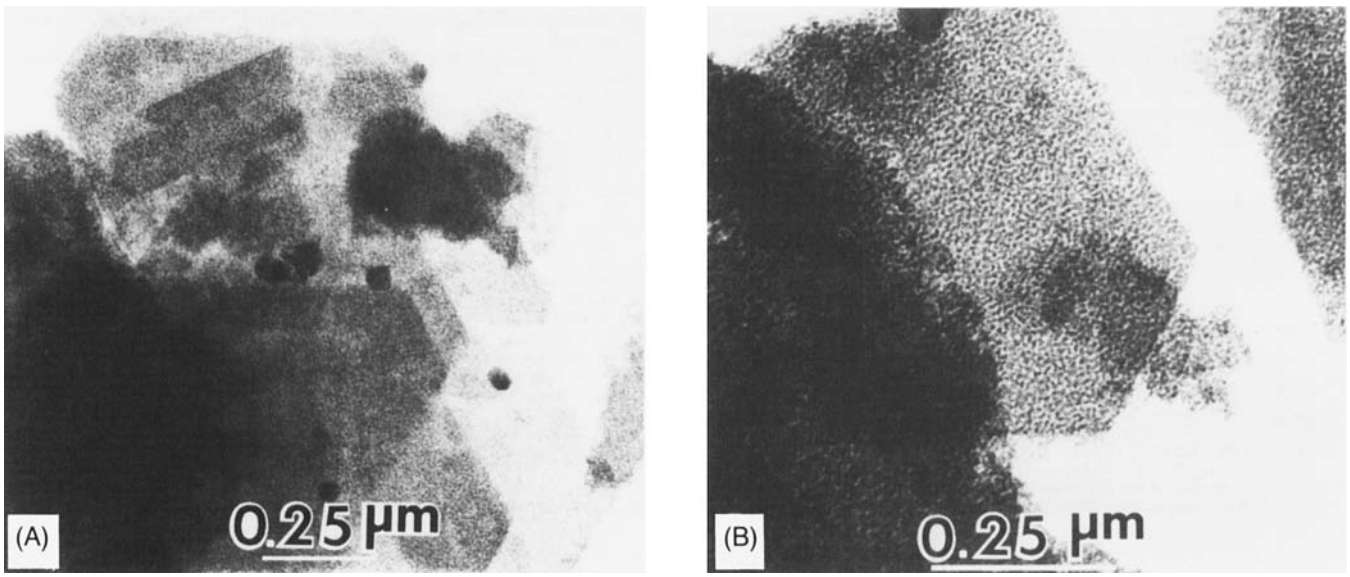

Fig. 5. (*A*) and (*B*) are BF images of the sample heat-treated at 850°C (1 week) and leached with NaOH to isolate the spinel phase. Images were taken under slightly underfocused condition to reveal small-scale crystals (dark contrast) and pores (light contrast) left after the removal of the matrix SiO_2 phase.

changed through a possible reaction with the leachant. These direct microanalysis results clearly disprove the validity of the previously reported Al-Si spinel models with significantly higher (>28 wt%) silica contents.[13,16] On the other hand, these leaching experiments do not eliminate the possibility that the spinel phase might actually contain <10 wt% silica if the amount measured by EDS included some contribution from the surrounding (unleached) amorphous silica.

It should be emphasized that as the leaching time is extended, the amount of SiO_2 left in the structure decreases, although less so as the leaching time is prolonged. The important question is whether this SiO_2 is in solution in the spinel phase or it is left between the spinel regions which are still intact. Assuming that treating with NaOH only affects the SiO_2 layer between the spinel grains but does not readily affect the layers trapped between the two spinel grains, we calculated the amount of silica, at a thickness of 0.25 nm, that may still be present between closely packed particles of 5 to 8 nm in size to be nearly 10 wt%. The close agreement between this calculated value and the amount determined by EDS analysis then supports the view that the actual amount of silica could be <10 wt%. This argument is also supported by the fact that by prolonged leaching treatment the amount of SiO_2 continuously decreases, although the rate is very small. In fact, as evidenced in some EDS experiments performed on

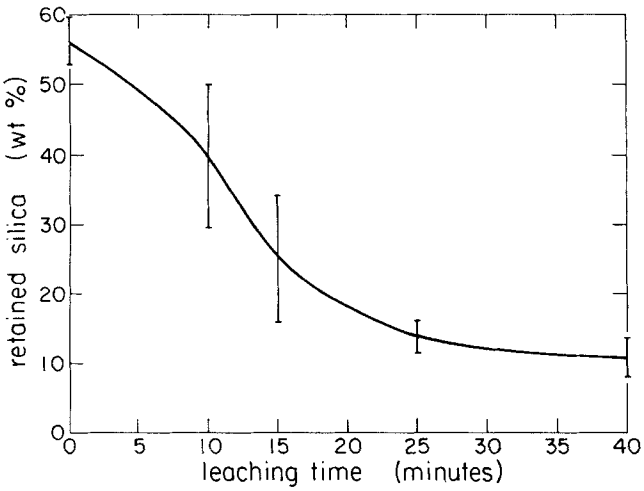

Fig. 6. The amount of silica left in the spinel-containing specimen as a function of leaching time. The wt% silica was calculated from the amount of Si measured by using EDS analysis in the TEM.

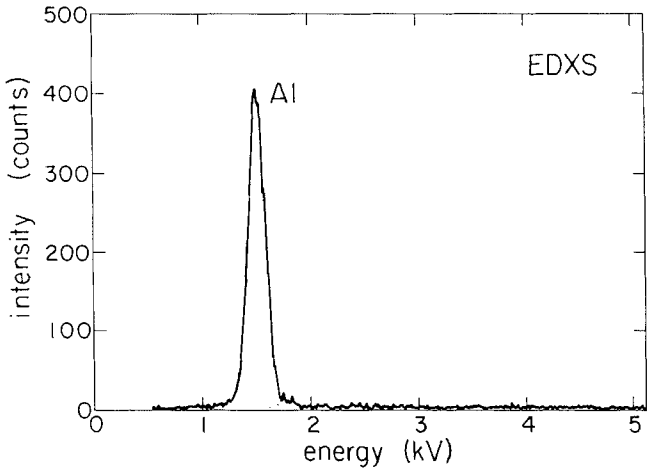

Fig. 7. An energy dispersive X-ray spectrum received from a spinel crystal formed in a sample heated in the vicinity of 980°C. Only the Al peak is observed, and almost no Si is present in the structure.

occasional spinel particles suspended at the edge of the powders (similar to the ones shown in Figs. 4 and 5, but now in the leached sample), we obtained EDS spectra which displayed only Al peak, and a negligibly small Si peak (Fig. 7).

IV. Conclusions

The main conclusion of this work is that the 980°C exotherm in the kaolinite-to-mullite reaction series is caused by the formation of a spinel phase but not by the parallel formation of spinel and mullite as reported in previous studies.[3,14,16] It is also concluded that this spinel contains not more than 10 wt% silica (if any).

Acknowledgments: We are grateful to G. Thomas for the use of the TEM facilities at the University of California, Berkeley. The initial part of this work on the differential thermal analysis was performed at the Middle East Technical University, Ankara, Turkey.

References

[1]H. LeChatelier, "The Effect of Heat on Clay" (in Fr.), *Bull. Soc. Fr. Mineral.*, **10**, 204–11 (1887).
[2]K. J. D. MacKenzie, I. W. M. Brown, R. H. Meinhold, and M. E. Bowden, "Outstanding Problems in the Kaolinite-Mullite Reaction Sequence Investigated by ^{29}Si and ^{27}Al Solid-State Nuclear Magnetic Resonance: I, Metakaolinite," *J. Am. Ceram. Soc.*, **68** [6] 293–97 (1985).
[3]I. W. M. Brown, K. J. D. MacKenzie, M. E. Bowden, and R. H. Meinhold, "Outstanding Problems in the Kaolinite-Mullite Reaction Sequence Investigated by ^{29}Si and ^{27}Al Solid-State Nuclear Magnetic Resonance: II, High Temperature Transformations of Metakaolinite," *J. Am. Ceram. Soc.*, **68** [6] 298–301 (1985).
[4]A. K. Chakravorty, D. K. Ghosh, and P. Kundu, "Comment on Structural Characterization of Spinel Phase in the Kaolin-Mullite Reaction Series through Lattice Energy," *J. Am. Ceram. Soc.*, **69** [8] C-200–C-201 (1986).
[5]S. Mazumdar and B. Mukherjee, "Reply to 'Comment on Structural Characterization of Spinel Phase in the Kaolin-Mullite Reaction Series through Lattice Energy,'" *J. Am. Ceram. Soc.*, **69** [8] C-201 (1986).
[6]A. K. Chakravorty and D. K. Ghosh, "Comment on Diphasic Xerogels, A New Class of Materials: Phases in the System Al_2O_3-SiO_2," *J. Am. Ceram. Soc.*, **69** [8] C-202–C-203 (1986).
[7]S. Komarneni and R. Roy, "Reply to 'Comment on Diphasic Xerogels, A New Class of Materials: Phases in the System Al_2O_3-SiO_2,'" *J. Am. Ceram. Soc.*, **69** [8] C-204 (1986).
[8]C. S. Ross and P. F. Kerr, The Kaolin Mineral. U.S. Geological Survey Progress Paper, No. 165E, 1930.
[9]H. Insley and R. H. Ewell, "Thermal Behavior of Kaolin Minerals," *J. Res. Natl. Bur. Stand.*, **14** [5] 615–27 (1935).
[10]J. E. Comefore, R. B. Fischer, and W. F. Bradley, "Mullitization of Kaolinite," *J. Am. Ceram. Soc.*, **31** [9] 254–59 (1948).
[11]W. F. Bradley and R. E. Grim, "High Temperature Thermal Effects of Clay and Related Minerals," *Am. Mineral.*, **36**, 182–201 (1951).
[12]R. Roy, D. M. Roy, and E. E. Francis, "New Data on Thermal Decomposition of Kaolinite and Halloysite," *J. Am. Ceram. Soc.*, **38** [6] 198–205 (1955).
[13]G. W. Brindley and M. Nakahira, "The Kaolinite-Mullite Reaction Series: I–III," *J. Am. Ceram. Soc.*, **42** [7] 311–24 (1959).
[14]H. J. Percival, J. F. Duncan, and P. K. Foster, "Interpretation of the Kaolinite-Mullite Reaction Sequence from Infrared Absorption Spectra," *J. Am. Ceram. Soc.*, **57** [2] 57–61 (1974).
[15]A. J. Leonard, "Structural Analysis of the Transition Phases in the Kaolinite to Mullite Thermal Sequence," *J. Am. Ceram. Soc.*, **60** [1–2] 37–43 (1977).
[16]A. K. Chakraborty and D. K. Ghosh, "Reexamination of the Kaolinite to Mullite Reaction Series," *J. Am. Ceram. Soc.*, **61** [3–4] 170–73 (1978).
[17]B. Sonuparlak, "Examination of Kaolinite to Mullite Reaction Series"; Ph.D. Thesis. Middle East Technical University, Ankara, Turkey, 1983.
[18]G. Cliff and G. W. Lorimer, "The Quantitative Analysis of Thin Specimens," *J. Microsc.*, **103**, 203–207 (1975).
[19]J. D. C. McConnell and S. G. Fleet, "Electron Optical Study of the Thermal Decomposition of Kaolinite," *Clay Miner.*, **8**, 279–90 (1970). □